ORGANIC CHEMISTRY

Accelerating reaction generality and mechanistic insight through additive mapping

Cesar N. Prieto Kullmer[1]†, Jacob A. Kautzky[1]†, Shane W. Krska[2], Timothy Nowak[3], Spencer D. Dreher[2]*, David W. C. MacMillan[1]*

Reaction generality is crucial in determining the overall impact and usefulness of synthetic methods. Typical generalization protocols require a priori mechanistic understanding and suffer when applied to complex, less understood systems. We developed an additive mapping approach that rapidly expands the utility of synthetic methods while generating concurrent mechanistic insight. Validation of this approach on the metallaphotoredox decarboxylative arylation resulted in the discovery of a phthalimide ligand additive that overcomes many lingering limitations of this reaction and has important mechanistic implications for nickel-catalyzed cross-couplings.

Over the past century, organic chemists have invented a substantial number of catalytic bond–forming reactions (Fig. 1A). Many of these innovative transformations enable streamlined access to high-value molecular motifs. However, despite the vast and growing body of known chemical reactions, only a select few are routinely used by organic chemists and researchers in adjacent fields. Among these are olefin metathesis, the Suzuki coupling, and the Buchwald-Hartwig coupling (*1*–*3*).

The few transformations that have made the leap from invention to mainstay reaction share a key feature: They are high yielding and robust and capable of readily accommodating a wide range of substrate functionality and complexity. It is generally accepted that the elusive attributes of substrate generality and reaction efficiency cannot be anticipated, and it typically takes years of rigorous study to fully optimize the scope and yield of a challenging reaction (*1*–*7*). As outlined in Fig. 1, traditional reaction generalization is an iterative process that begins with careful mechanistic investigation. The insights gained in this exercise may suggest rational modifications that can lead to incrementally improved performance through elaborate catalyst optimization (*8*–*14*). Unfortunately, this approach becomes problematic when applied to inherently complex catalytic systems, in which mechanistic insights into underlying issues are not straightforwardly achieved or leveraged (hereafter referred to as complex reactions). As a result, the chemical literature is replete with promising but underutilized reactions that have yet to realize their full potential because of their mechanistic ambiguity.

In response to this challenge, we sought to develop an approach amenable to the generalization of complex reactions that also yields mechanistic insight that is inaccessible otherwise. Inspiration was drawn from the medicinal chemistry practice of phenotypic screening (*15*–*19*). A phenotypic screen involves the application of libraries of chemically diverse compounds to entire biological systems of interest while searching for desirable changes in the observable traits (the phenotype). This approach has the potential to simultaneously uncover and modulate hitherto unrecognized biomolecular mechanisms. It has proven invaluable in developing powerful therapeutic approaches that leverage unappreciated mechanisms of action and improved indications recalcitrant to traditional drug discovery techniques (*20*–*23*). We reasoned that complex reactions can be likened to complex biological systems, so there would be enormous benefit to applying this concept to the study and improvement of the former.

Unexpected improvements in reaction efficiency achieved with additives is a well-documented but often overlooked phenomenon within organic chemistry. Examples include the lithium chloride effect in Stille couplings (*24*) and, more recently, work conducted by the Watson group (*25*), the Dong group (*26*), and our own groups (*27*, *28*). Discovered additives can often be rationalized ex post facto but are nearly impossible to predict a priori. More importantly, knowledge of additive effects can be leveraged to extract important information about the mechanism of the reaction itself. Rapid evaluation of an additive library might therefore result in similar unforeseen mechanistic modifications that benefit the reaction and lead to important mechanistic insights.

Our envisioned strategy is outlined in Fig. 1 (bottom). We selected a challenging, complex reaction of limited substrate scope and began evaluating additives in a systematic fashion. Using high-throughput experimentation (HTE) methods, we were able to identify privileged motifs by mapping the evaluated additive space onto the resulting yield. Identified hits were then evaluated through structure-activity relationship (SAR) and mechanistic studies with the goal of identifying the optimal additive and gaining broader chemical insights. Rationalization of the additive effect should generate new, nonobvious mechanistic information useful to organic methodology at large.

We sought to apply this approach to the construction of $C(sp^2)$–$C(sp^3)$ bonds in an effort to forward the long-sought-after goal to "escape from flatland" within contemporary drug discovery (*29*, *30*). Several elegant methods have been developed to address this gap, but none has the requisite starting material availability to enable broad access to chemical space (*31*–*37*). The metallaphotoredox decarboxylative arylation reaction initially published by the Doyle and MacMillan groups (*38*) has the putative advantage of broad commercial availability of both substrates (carboxylic acid and aryl halide) but has not gained widespread traction because of shortcomings in reaction generality. Specifically, the decarboxylative arylation is not amenable to (i) coordinating substrates, (ii) aryl bromides prone to protodehalogenation, (iii) challenging oxidative additions, or (iv) nonactivated carboxylic acids—namely, those that result in unstabilized radicals upon oxidative decarboxylation (*39*). Major efforts by our group and others (*40*) using traditional optimization approaches have failed to either substantially expand the scope of this reaction or to yield any helpful mechanistic leads. Therefore, our additive mapping approach could be well equipped to address this challenge.

To begin, we focused on an additive library of 721 diverse organic molecules amenable to HTE evaluation (Fig. 2B; also see the supplementary materials for further discussion). In principle, this approach should also be compatible with other classes of additives (e.g., salts, ligands, and metals). Concomitantly, we also selected several challenging coupling partners, including substrates with coordinating basic nitrogens, nonactivated carboxylic acids, and aryl halides that lead to sizeable quantities of Minisci and protodehalogenation side products. These reactions were performed in a nanomole-scale photoredox setup in which performance, as determined by reaction yield, was evaluated in the presence of each additive.

Unsurprisingly, most additives, particularly those containing groups such as heterocycles, anilines, and phenols, led to attenuated reaction efficiency (*41*) (Fig. 2B). However, certain five-membered cyclic imides and hydantoins were found to give a strong boost

[1]Merck Center for Catalysis at Princeton University, Princeton, NJ 08544, USA. [2]Department of Process and Analytical Chemistry, MRL, Merck & Co., Inc., Rahway, NJ 07065, USA. [3]Department of Discovery Chemistry, MRL, Merck & Co., Inc., Kenilworth, NJ 07033, USA.
*Corresponding author. Email: dmacmill@princeton.edu (D.W.C.M.); spencer_dreher@merck.com (S.D.D.)
†These authors contributed equally to this work.

in overall yield, sometimes up to fivefold, as well as a sharp decrease in protodehalogenation. This result was unexpected given that coordinating functionality is traditionally a powerful reaction poison caused by catalyst chelation.

Further evaluation of these unexpected hits was done using SAR studies. A total of 48 substrate combinations (three acids against 16 aryl bromides) were selected and evaluated on a nanoscale against 64 commercially available imide and hydantoin additives (Fig. 2C, left, and figs. S10 and S11). Substrate-dependent improvements were seen for a range of additives, but phthalimide proved to be the most broadly applicable. It generally gave the largest yield improvement, was commercially available, and was easily removed during workup. Methylation of the nitrogen, installation of electron-deficient substituents on the aromatic ring, or alteration of the five-membered ring size impaired or completely ablated the observed improvement. The steric effects of the imide additive, however, proved unimportant, with even tetramethylsuccinimide performing well.

To gauge improvements in the functional group tolerance, compound X2 and cyclohexanoic acid were resubjected to the earlier additive screen in the presence of phthalimide, and overall reaction performance was substantially better (Fig. 2C, right, and fig. S13). A range of compounds that previously served as reaction poisons (e.g., 1,3-dicarbonyls and benzoic acids) were now well tolerated. Furthermore, examining the data in aggregate showed that the overall average yield nearly doubled in the presence of phthalimide, and the overall number of reaction poisons (defined as decreasing the yield by >33%) fell from 390 to 208.

With these exciting results in hand, we sought to benchmark the reaction improvement in a pharmaceutically relevant context against the Aryl Halide Informer Library (*42*). This library is prototypical of the type of complex drug-like compounds seen in medicinal chemistry and contains a range of (hetero)aryl halides deemed to be inherently challenging for metal-catalyzed cross-couplings. When evaluating the library against a nonactivated acid, we found that phthalimide had an outstanding impact. A sizeable 11 of the 18 aryl halides showed major performance improvements, and a tripling of overall average yield was observed, from 7.7 to 29.4% (Fig. 3A and fig. S14). Failures included compounds with free carboxylic acids (X7 and X9) and aryl chlorides (X16 to X18), substrates that lie outside the scope of this transformation. The results position the decarboxylative arylation among the most successful couplings evaluated against the library.

Encouraged by the informer results, we then set our sights on evaluating the new scope of

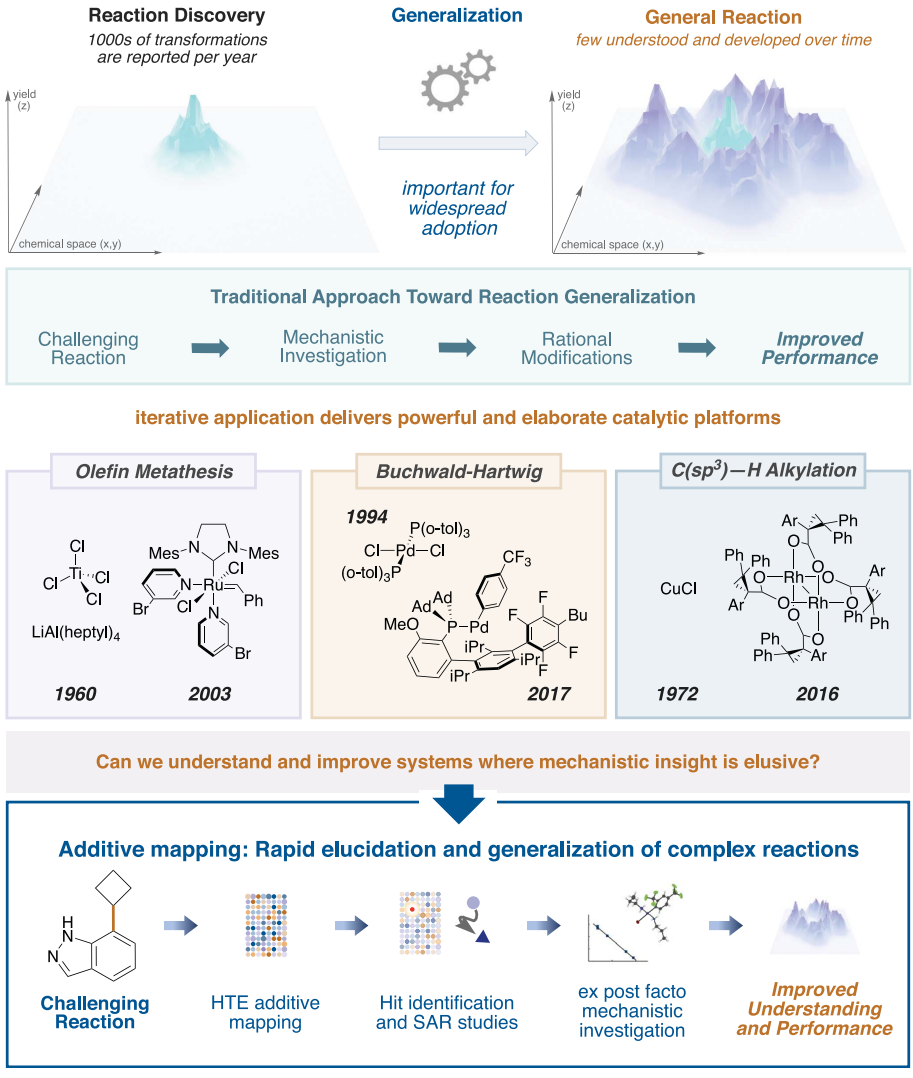

Fig. 1. High-throughput additive mapping to understand and improve organic methods. Shown are the traditional approach and select successes, as well as the proposed HTE additive mapping approach.

the reaction using the phthalimide additive. A highly diverse array of 384 small, medicinally relevant aryl bromides were evaluated against a complex, nonactivated isonipecotic acid derivative on a nanomole scale (see the supplementary materials for details). To gauge the synthetic utility of the phthalimide additive, we used charged aerosol detection (CAD) to determine the yield of each reaction (*43*). A 10% reaction yield was selected as threshold for the potential isolability of products by mass-directed microisolation that was based on prior work (*44*, *45*).

With phthalimide, the number of compounds above our typical threshold for isolation more than doubled, from 70 to 187 (Fig. 3B, right, and fig. S17). Substantial improvements were observed for a wide variety of bromides, including six-membered ring systems (aryl bromides, pyridines, and pyrimidines), five-membered heterocycles (pyrazoles, imidazoles, and thiazoles), and [6,5]- and [6,6]-heterobicycles (indoles, aza-indoles, benzimidazoles, and quinolines). Furthermore, phthalimide improved the functional group compatibility of the reaction, allowing for the presence of polar moieties such as 1,2-diols, phenols, and aminopyridines.

We next examined the scope of 384 chemically diverse, relevant carboxylic acids against the structurally complex informers X1, X2, and X13 on a nanomole scale (1152 total combinations). The phthalimide additive produced important improvements in a range of primary carboxylic acids including alpha ether, alpha thioether, benzylic, and, most notably, nonactivated acids, the latter representing a crucial advancement in overall reaction generality because they were previously only narrowly tolerated (Fig. 3B, left, and figs. S21 to S23). Further improvements were likewise seen for a range of cyclic carboxylic acids,

including both activated and nonactivated four-, five-, six-, and seven-membered rings. A boost in yield was also seen for a range of acyclic carboxylic acids, and 19 of 20 protected amino acids were cross-coupled successfully in the presence of phthalimide, including both potential sites in aspartic acid and glutamic acid. Finally, the overall functional group compatibility of the reaction appeared far more robust in the presence of phthalimide. Substrates bearing a range of functionalities, including phenols, aldehydes, aryl chlorides, and β-alcohols, performed notably better with the additive. In aggregate, the number of reactions delivering products in >10% yields increased from 212 to 516, and the overall reaction CAD yield across the set increased more than twofold. The improvements in both aryl bromide and acid scope observed in this study should, in a realistic setting, have a large impact on the generality of the decarboxylative arylation in synthesis at large.

With these marked improvements in hand, we next sought to leverage the discovered effect of phthalimide to generate a fundamental mechanistic understanding useful for future Ni-metallaphotoredox developments. We first focused on elucidating how phthalimide turns nonactivated acids into competent coupling partners. Evaluating the reaction progress of a model system (figs. S31 and S32; substrate pair yields were 23% without phthalimide and 81% with phthalimide), we observed

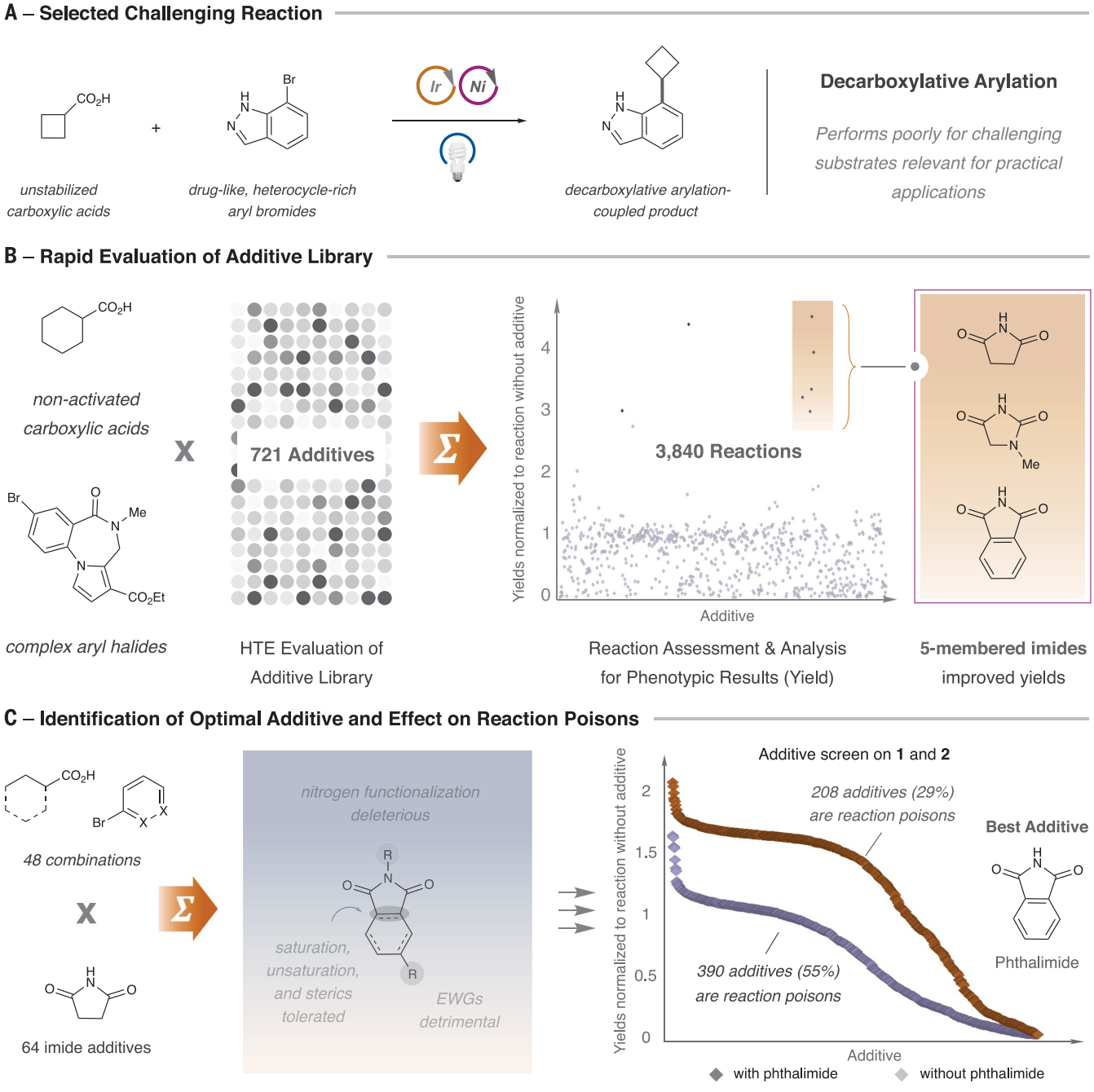

Fig. 2. Additive mapping applied to the decarboxylative reaction. (**A**) Metallaphotoredox decarboxylative arylation. (**B**) High-throughput additive screening on challenging coupling partners revealing the imide effect. (**C**) Left: SAR studies to identify the ideal five-membered imide. A set of 64 imides was evaluated in 48 couplings to reveal the best imide. Right: Phthalimide can counteract the poisoning effect of problematic functionalities.

full consumption of the aryl bromide and substantial protodehalogenation in the absence of phthalimide. Conversely, suppression of protodehalogenation and predominant formation of the desired cross-coupled product was observed in the presence of phthalimide. We hypothesized that phthalimide prevents the decomposition of the intermediate oxidative addition complex (OAC), the most likely source of protodehalogenation.

To investigate the possibility of a stabilizing interaction between the putative Ni-aryl complex and phthalimide in the reaction, we sought to emulate the formation of such a complex under reaction-relevant conditions. The Ni(II) precatalyst was reduced by dropwise addition of $(Cp^*)_2Co$ in the presence of carboxylic acid, 2-tert-butyl-1,1,3,3-tetramethylguanidine

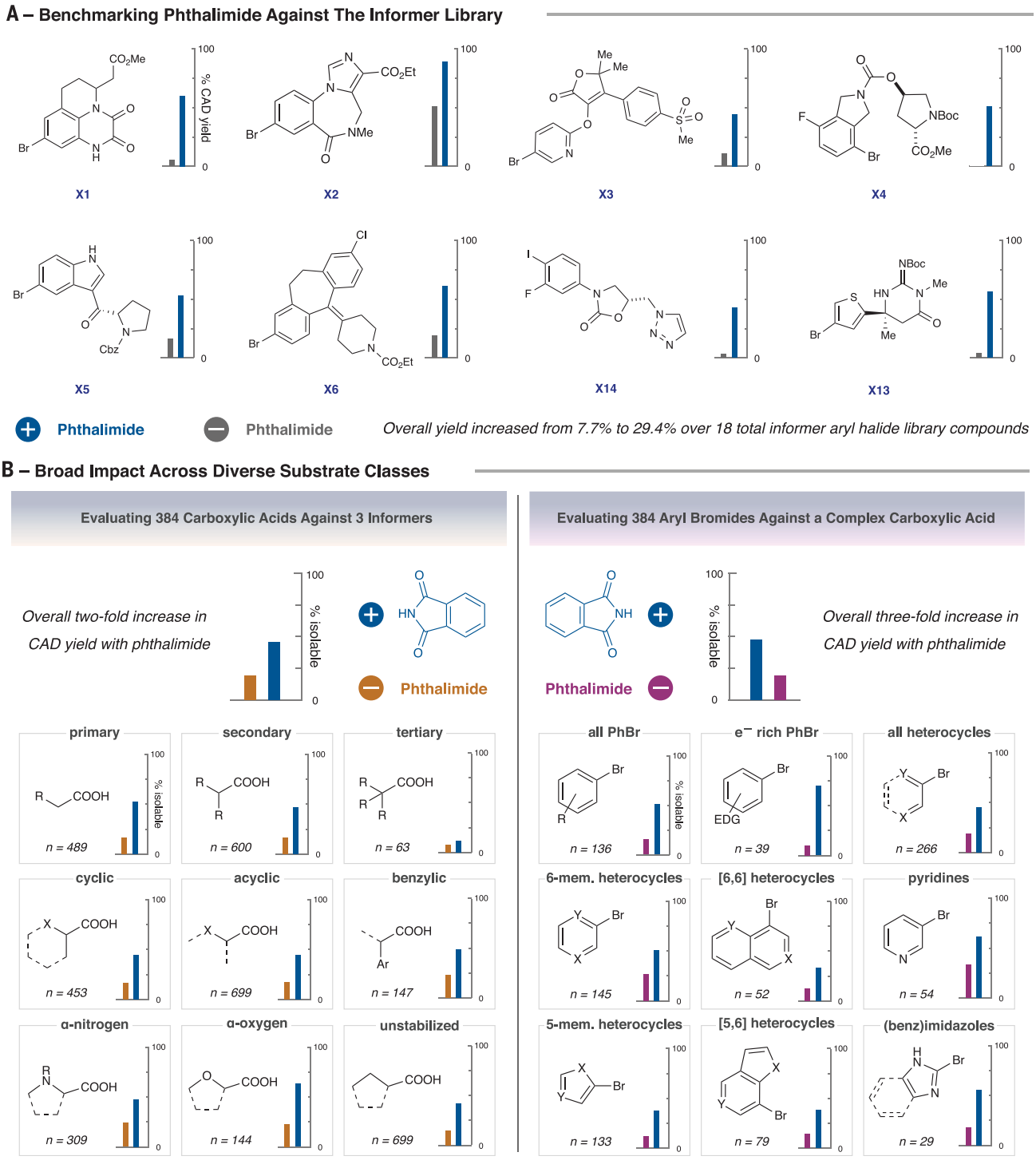

Fig. 3. Scope of the decarboxylative arylation. (**A**) Scope of the Aryl Halide Informer Library investigated against tetrahydropyran-4-carboxylic acid (% CAD yield reported). (**B**) Nanoscale high-throughput scope evaluation (% isolable reported). A product is deemed isolable if the CAD yield is ≥10%. *n*, number of evaluated compounds in this category; EDG, electron-donating group.

(BTMG), and aryl bromide (Fig. 4B). We found that in the presence of potassium phthalimide, an OAC was formed that persisted for several hours [as determined by ^{19}F-nuclear magnetic resonance (^{19}F-NMR) characterization], whereas in absence of phthalimide, we obtained only protodehalogenation and reductive homocoupling products. The identity of the observed OAC was subsequently confirmed through independent synthesis.

Isolated complex ***3*** has substantial stability, which stands in stark contrast to the typically rapid decomposition of OACs lacking ortho substituents on the aryl ligand (*46*). Complex ***3*** is stable for at least 24 hours in the dark in both dimethyl sulfoxide (DMSO) and dichloromethane (DCM), as well as under irradiation for 2 hours in DMSO. Under reaction-relevant conditions, we found that decomposition was prevented when an excess of potassium phthalimide was added to prevent ligand exchange by carboxylates. Phthalimide thus likely precludes typical decomposition pathways by keeping complex ***3*** coordinatively saturated. Despite this inherent stability, complex ***3*** is fully able to capture radicals and undergo reductive elimination to form the desired cross-coupled product. Irradiation of complex ***3*** in the presence of an equimolar amount of $(Ir[dF(CF_3)ppy]_2(dtbpy))PF_6$ and excess of carboxylic acid, BTMG, and potassium phthalimide yields the desired cross-coupled product in 67% yield (see the supplementary materials).

We then set out to probe the importance of complex ***3*** to the reaction itself. Evaluation of the reaction progress of an activated acid (N-benzyloxycarbonyl-proline) and a nonactivated acid (cyclopentanoic acid) in the presence of phthalimide revealed that the nonactivated acid reacted more slowly overall (Fig. 4B, left). A Stern-Volmer analysis revealed a clear difference in the photocatalyst quenching rate between the two acids (Fig. 4B, middle). The slower quenching of nonactivated acids translates not only into slower formation of alkyl radicals but also slower formation of reduced iridium photocatalyst. By extension, we reasoned that this leads to slower Ni reduction and slower formation of the OAC. The lower steady-state concentration of alkyl radicals and OACs translates into a slower rate of radical capture by Ni, which allows for it to be outcompeted by the unimolecular OAC decomposition pathway. Stabilizing the OAC should therefore benefit nonactivated acids because it precludes the decomposition pathway and extends the time frame for successful radical capture. A PhotoNMR experiment (using cyclopentanoic acid) in the absence of phthalimide revealed no ^{19}F-NMR signals that could be assigned to an OAC. When this experiment was repeated in the presence of phthalimide, a new ^{19}F-NMR signal was observed that matched the signal obtained from complex ***3***, indicating a considerable increase in the steady-state concentration of the OAC (Fig. 4B, right). This further supports our hypothesis.

Along a different line of inquiry, we realized that electron-rich aryl bromides seemed to give particularly strong improvements in yield, and we suspected a correlation between the electronic properties of the aryl group and the effect of phthalimide. A Hammett study was conducted both in absence and in presence of phthalimide to probe this hypothesis (Fig. 4C, left). A moderately strong Hammett ρ of 1.57 was observed in the absence of phthalimide, which suggests that the oxidative addition of the aryl bromide contributes to the overall rate of the reaction. We found that the addition of phthalimide led to an overall increase in the initial reaction rate, in particular for electron-rich aryl bromides, and a lowered ρ of 0.56. We reasoned here that phthalimide must have some bearing on the oxidative addition.

To uncover the specific role of phthalimide in the oxidative addition, we evaluated the progress of a different model catalytic reaction in the presence and absence of phthalimide (Fig. 4C, top; substrate pair yields were 10% without phthalimide and 70% with phthalimide). Unexpectedly, in the absence of phthalimide, the reaction underwent deactivation over the first 100 min to reach an unproductive stationary state, whereas in the presence of phthalimide, the reaction steadily went to completion (figs. S24 and S25). In conjunction with the Hammett data, we found it reasonable to postulate a deactivation of the reaction caused by a progressive decrease in catalytically active Ni able to undergo oxidative addition. Phthalimide would thus act by bringing the Ni back on cycle.

To investigate the reactivation hypothesis, a competition study between phenyl bromide and various electronically distinct aryl bromides was conducted to assess product ratios at an early time point both in absence and presence of phthalimide (see the supplementary materials for details). For each aryl bromide, we found that product ratios did not change meaningfully when phthalimide was added (with the exception of the electron-poor 4-bromobenzotrifluoride). This is consistent with the hypothesis that phthalimide serves to increases the amount of Ni competent to undergo oxidative addition, which supports the proposed reactivation hypothesis.

It was reasonable to hypothesize that the deactivation could be attributed to the formation of low-valent Ni oligomers, which are known to be unreactive toward oxidative addition in their oligomeric form (*47*, *48*). Independently prepared dimer $[(dtbbpy)NiBr]_2$ was subjected to the reaction to test this hypothesis (Fig. 4C, middle). Trace yield of product was observed with the dimer for the previously used substrate pair, which confirms that this Ni species by itself is incompetent in this reaction. Repeating this experiment in the presence of phthalimide afforded the product in 31% yield, thus demonstrating that phthalimide can, at least in principle, return unreactive multimers into a monomeric, catalytically active state. Stable (bpy)Ni(I)-phthalimido complexes have been reported, which lends support to this hypothesis (*49*).

Taking the previous observations together, we reasoned that the addition of phthalimide to a deactivated reaction should lead to a reactivation of the catalysts and resumption of product formation. Phthalimide should break up any formed inactive multimeric species and thus allow for productive turnover. Consistent with our hypothesis, when phthalimide was doped into such a reaction, we observed almost complete reactivation and steady turnover (Fig. 4C, right).

Overall, we believe that phthalimide acts in two mechanistically distinct manners. First, phthalimide affects the stability of Ni-aryl complexes by acting as a ligand that precludes decomposition pathways such as protodehalogenation and aryl metathesis. This also accounts for the inclusion of nonactivated acids into the scope of this transformation, where the increased OAC lifetime counteracts the lower effective radical concentration inherent to these acids. Furthermore, when using electron-rich aryl bromides, the reaction undergoes reversible deactivation caused by a decrease in the effective concentration of on-cycle Ni catalyst. This is presumably because of the formation of off-cycle, unreactive multimeric species resulting from the aggregation of low-valent Ni complexes. Phthalimide is capable of reactivating inactive multimeric Ni species and thus increasing the concentration of catalytically active Ni, which allows the catalytic cycle to be productively turned over. We do not rule out further effects of phthalimide in this reaction, and additional mechanistic investigations are currently ongoing. The effect of phthalimide on Ni-catalyzed cross-couplings in general is also undergoing further investigation.

In summary, by identifying phthalimide as a beneficial additive for decarboxylative arylation, we were able to develop a general transformation to reliably form $C(sp^2)$–$C(sp^3)$ bonds from feedstock chemicals. This improvement was achieved in less than a year from project inception, which highlights the expedited nature of additive mapping. Furthermore, we then leveraged the discovered phthalimide effect to broaden the mechanistic understanding of Ni-catalyzed cross-coupling from an angle not accessible by traditional mechanistic studies, which highlights the orthogonality of this approach. We imagine that both the use of phthalimide as an additive and the herein

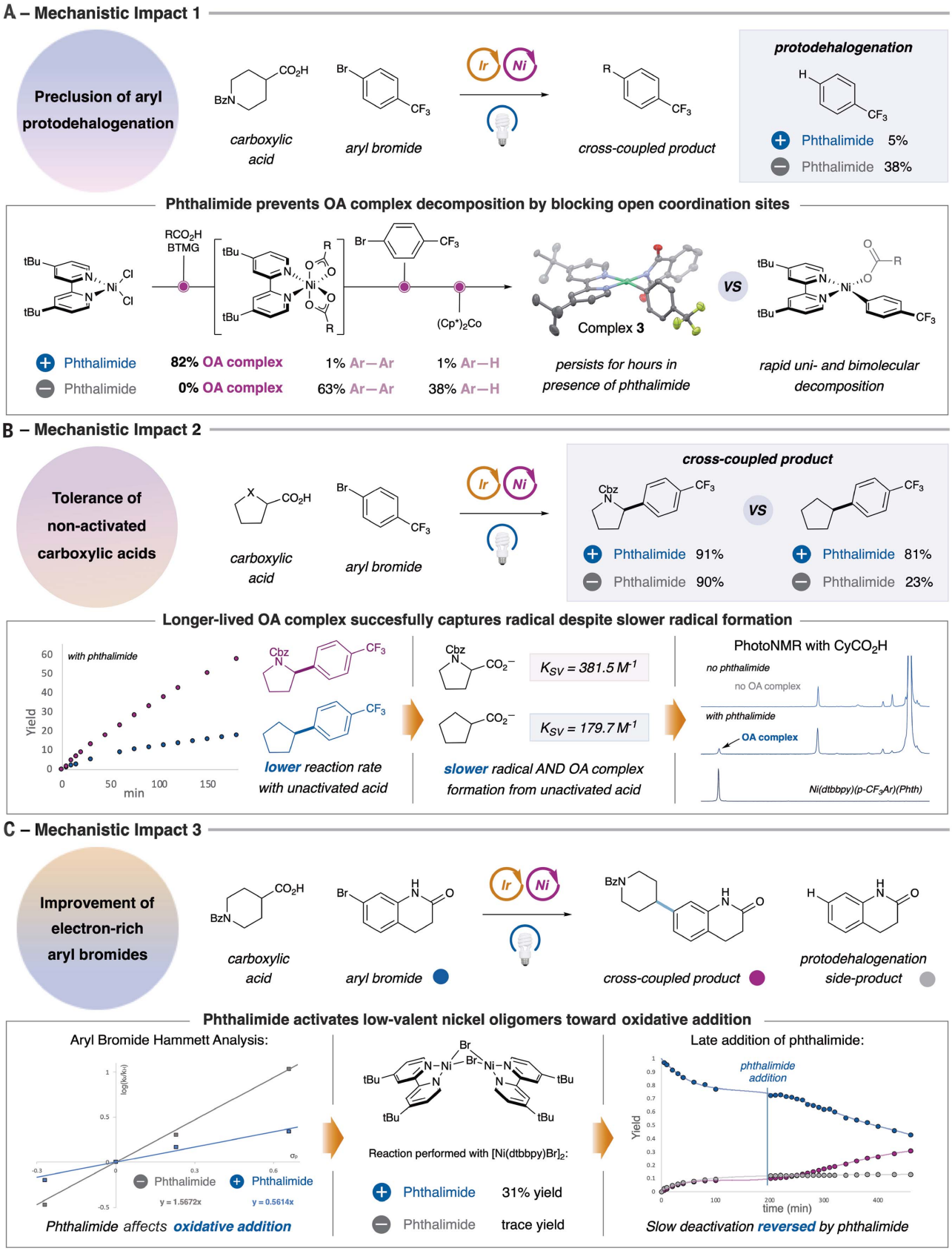

Fig. 4. Mechanistic insight. (**A**) Decrease of protodehalogenation observed with phthalimide caused by stabilization of the OAC. For the x-ray structure (50% probability ellipsoids), hydrogens and tBu/CF3 disorder are omitted for clarity. (**B**) Slower quenching is tolerated because of the increased OAC concentration. (**C**) Increasing active Ni on cycle by activation of low-valent Ni oligomers.

reported approach for reaction generalization and mechanistic elucidation will be rapidly embraced to affect modern organic synthesis.

REFERENCES AND NOTES

1. T. M. Trnka, R. H. Grubbs, *Acc. Chem. Res.* **34**, 18–29 (2001).
2. N. Miyaura, A. Suzuki, *Chem. Rev.* **95**, 2457–2483 (1995).
3. P. Ruiz-Castillo, S. L. Buchwald, *Chem. Rev.* **116**, 12564–12649 (2016).
4. H. C. Brown, *Hydroboration* (W. A. Benjamin, 1962)
5. J. Tsuji, *Palladium Reagents and Catalysts* (Wiley, 1995)
6. C. C. C. Johansson Seechurn, M. O. Kitching, T. J. Colacot, V. Snieckus, *Angew. Chem. Int. Ed.* **51**, 5062–5085 (2012).
7. Y. Park, Y. Kim, S. Chang, *Chem. Rev.* **117**, 9247–9301 (2017).
8. W. L. Truett, D. R. Johnson, I. M. Robinson, B. A. Montague, *J. Am. Chem. Soc.* **82**, 2337–2340 (1960).
9. T. L. Choi, R. H. Grubbs, *Angew. Chem. Int. Ed.* **42**, 1743–1746 (2003).
10. A. S. Guram, S. L. Buchwald, *J. Am. Chem. Soc.* **116**, 7901–7902 (1994).
11. F. Paul, J. Patt, J. F. Hartwig, *J. Am. Chem. Soc.* **116**, 5969–5970 (1994).
12. B. T. Ingoglia, S. L. Buchwald, *Org. Lett.* **19**, 2853–2856 (2017).
13. R. T. Conlin, P. P. Gaspar, R. H. Levin, M. Jones Jr., *J. Am. Chem. Soc.* **94**, 7165–7166 (1972).
14. K. Liao, S. Negretti, D. G. Musaev, J. Bacsa, H. M. L. Davies, *Nature* **533**, 230–234 (2016).
15. J. A. Lee, M. T. Uhlik, C. M. Moxham, D. Tomandl, D. J. Sall, *J. Med. Chem.* **55**, 4527–4538 (2012).
16. J. G. Moffat, F. Vincent, J. A. Lee, J. Eder, M. Prunotto, *Nat. Rev. Drug Discov.* **16**, 531–543 (2017).
17. B. K. Wagner, S. L. Schreiber, *Cell Chem. Biol.* **23**, 3–9 (2016).
18. D. G. Brown, H. J. Wobst, *J. Med. Chem.* **63**, 1823–1840 (2020).
19. W. Zheng, N. Thorne, J. C. McKew, *Drug Discov. Today* **18**, 1067–1073 (2013).
20. D. C. Swinney, J. Anthony, *Nat. Rev. Drug Discov.* **10**, 507–519 (2011).
21. Q. T. L. Pasquer, I. A. Tsakoumagkos, S. Hoogendoorn, *Molecules* **25**, 5702–5724 (2020).
22. W. Dejonghe, E. Russinova, *Plant Physiol.* **174**, 5–20 (2017).
23. M. Szabo *et al*., *Drug Des. Devel. Ther.* **11**, 1957–1967 (2017).
24. A. L. Casado, P. Espinet, A. M. Gallego, *J. Am. Chem. Soc.* **122**, 11771–11782 (2000).
25. J. C. Vantourout, H. N. Miras, A. Isidro-Llobet, S. Sproules, A. J. B. Watson, *J. Am. Chem. Soc.* **139**, 4769–4779 (2017).
26. Z. Dong, J. Wang, G. Dong, *J. Am. Chem. Soc.* **137**, 5887–5890 (2015).
27. A. Bellomo *et al*., *Angew. Chem. Int. Ed.* **51**, 6912–6915 (2012).
28. P. J. Sarver *et al*., *Nat. Chem.* **12**, 459–467 (2020).
29. F. Lovering, J. Bikker, C. Humblet, *J. Med. Chem.* **52**, 6752–6756 (2009).
30. W. P. Walters, J. Green, J. R. Weiss, M. A. Murcko, *J. Med. Chem.* **54**, 6405–6416 (2011).
31. R. Jana, T. P. Pathak, M. S. Sigman, *Chem. Rev.* **111**, 1417–1492 (2011).
32. C. Han, S. L. Buchwald, *J. Am. Chem. Soc.* **131**, 7532–7533 (2009).
33. N. Fleury-Brégeot *et al*., *J. Org. Chem.* **77**, 10399–10408 (2012).
34. L. Li, S. Zhao, A. Joshi-Pangu, M. Diane, M. R. Biscoe, *J. Am. Chem. Soc.* **136**, 14027–14030 (2014).
35. J. H. Kirchhoff, M. R. Netherton, I. D. Hills, G. C. Fu, *J. Am. Chem. Soc.* **124**, 13662–13663 (2002).
36. I. D. Hills, M. R. Netherton, G. C. Fu, *Angew. Chem. Int. Ed.* **42**, 5749–5752 (2003).
37. A. W. Dombrowski *et al*., *ACS Med. Chem. Lett.* **11**, 597–604 (2020).
38. Z. Zuo *et al*., *Science* **345**, 437–440 (2014).
39. J. Hioe, H. Zipse, *Org. Biomol. Chem.* **8**, 3609–3617 (2010).
40. R. W. Evans, *Novel Coupling Reactions Utilizing Base Metal and Photoredox Catalysis* (Princeton Univ. Press, 2017).
41. K. D. Collins, F. Glorius, *Nat. Chem.* **5**, 597–601 (2013).
42. S. D. Dreher, S. W. Krska, *Acc. Chem. Res.* **54**, 1586–1596 (2021).
43. N. Vervoort, D. Daemen, G. Török, *J. Chromatogr. A* **1189**, 92–100 (2008).
44. Products were identified using mass spectrometry and UV210 and UV250 signatures. Selected examples were scaled up to confirm product formation (see the supplementary materials).
45. K. D. Dykstra *et al*., *ACS Med. Chem. Lett.* **12**, 337–342 (2021).
46. T. Yamamoto, S. Wakabayashi, K. Osakada, *J. Organomet. Chem.* **428**, 223–237 (1992).
47. N. A. Till, S. Oh, D. W. C. MacMillan, M. J. Bird, *J. Am. Chem. Soc.* **143**, 9332–9337 (2021).
48. R. Sun *et al*., *J. Am. Chem. Soc.* **141**, 89–93 (2019).
49. B. Nestler, E. Uhlig, *Z. Anorg. Allg. Chem.* **530**, 196–206 (1985).

ACKNOWLEDGMENTS

We thank N. Till, P. Sarver, and Z. Dong for helpful discussions; T. Liu for support with graphic design; and P. Jeffrey for assistance with crystallography. The content is solely the responsibility of the authors and does not necessarily represent the official views of the National Institute of General Medical Sciences of the National Institutes of Health (NIH). **Funding:** This work was supported by the National Institute of General Medical Sciences of the National Institutes of Health (award R35GM134897-02) and by Merck Sharp & Dohme Corp., a subsidiary of Merck & Co., Inc.; Kenilworth, NJ, USA; Pfizer; Janssen; Bristol-Myers Squibb; Genentech; and Celgene. C.N.P.K. was supported by Princeton University, E. Taylor, and the Taylor family by an Edward C. Taylor fellowship. J.A.K. was supported by a predoctoral fellowship (award DGE 1656466) from the National Science Foundation. **Author contributions:** S.W.K., S.D.D., and D.W.C.M. conceived of the work. All authors designed the experiments. C.N.P.K., J.A.K., T.N., and S.D.D. performed and analyzed the experiments. C.N.P.K., J.A.K., S.W.K., S.D.D., and D.W.C.M. prepared the manuscript. **Competing interests:** D.W.C.M. declares a competing financial interest with respect to the integrated photoreactor (commercialized as PennPhD Photoreactor M2). The remaining authors declare no competing interests. **Data and materials availability:** Data are available in the supplementary materials. The Cambridge Crystallographic Data Centre (CCDC) website contains the supplementary crystallographic data for this paper, which can be obtained free of charge at www.ccdc.cam.ac.uk/data_request/cif under identifier 2153752.

SUPPLEMENTARY MATERIALS

science.org/doi/10.1126/science.abn1885
Materials and Methods
Supplementary Text
Figs. S1 to S35
NMR Spectral Data
References (*50*–*55*)
Excel Data for HTE Experiments
Data for Experiments 9.1 and 10.1 to 10.3

9 November 2021; accepted 25 March 2022
10.1126/science.abn1885

Science

Accelerating reaction generality and mechanistic insight through additive mapping

Cesar N. Prieto KullmerJacob A. KautzkyShane W. KrskaTimothy NowakSpencer D. DreherDavid W. C. MacMillan

Science, 376 (6592), • DOI: 10.1126/science.abn1885

Additive improvements to nickel catalysis

It often takes decades of incremental optimization to apply chemical reactions beyond the small range of substrates studied at the discovery stage. Prieto Kullmer *et al*. sought to accelerate that optimization process by screening a large, diverse group of additives to a cooperative nickel-photoredox catalyst system. The screen revealed that phthalimides substantially expand the functional compatibility of the nickel catalyst and thus the substrate scope. The phthalimide appears to stabilize oxidative addition complexes as well as break up deactivated catalyst aggregates. — JSY